Catalysis Letters 7 (1990) 183–196

STRUCTURE SENSITIVE REACTIONS OVER SUPPORTED RUTHENIUM CATALYSTS DURING FISCHER-TROPSCH SYNTHESIS

H. ABREVAYA, M.J. COHN, W.M. TARGOS (*UOP*) and H.J. ROBOTA (*Allied-Signal*)

UOP/Allied Signal, 50 E. Algonquin, DesPlaines, Illinois 60017, U.S.A.

Reverse micelle, Fischer-Tropsch, ruthenium, particle size, water-gas shift, dispersion, agglomeration.

Highly dispersed ruthenium catalysts can be prepared on alumina by aqueous impregnation of ruthenium. EXAFS at the K-edge showed that this type of catalyst, after calcination and reduction, consisted of ruthenium particles, which were about 0.8 nm in size. When highly dispersed on alumina, ruthenium appears to catalyze the water-gas shift reaction, which occurs subsequent to Fischer-Tropsch synthesis. The hydrocarbons produced had low olefinicity, possibly because of *in situ* production of hydrogen via the water-gas shift reaction. Highly dispersed ruthenium was not stable on alumina during Fischer-Tropsch synthesis. The ruthenium agglomeration on the alumina surface, as well as overall ruthenium loss from the catalyst, was attributed to the formation of a volatile ruthenium carbonyl species.

Catalysts with about 85% of the ruthenium in the form of 3–7 nm particles were prepared on alumina by reverse micelle impregnation of ruthenium. These larger particles were stable against ruthenium carbonyl formation and, therefore, did not exhibit ruthenium agglomeration or loss of ruthenium. Catalysts with 3–7 nm ruthenium particles displayed a higher turnover number for hydrocarbon synthesis, higher olefinicity, and chain-growth probability and did not exhibit water-gas shift activity in contrast to ruthenium particles which were about 0.8 nm in size.

The CO disproportionation measurements showed much less CO dissociation over highly dispersed ruthenium relative to 3–7 nm ruthenium particles. This phenomenon is consistent with the low activity, the low chain-growth probability and may also relate to the tendency to form ruthenium carbonyl that is observed with small ruthenium particles. The apparent water-gas shift activity of highly dispersed ruthenium can be explained by the low CO dissociation efficiency as well as by the proposed ability to dissociate the water molecule.

1. Introduction

The effects of metal particle size with supported ruthenium catalysts in Fischer-Tropsch synthesis have been previously reported [1–6]. Abrevaya et al. reported CO to undergo three different types of reactions during Fischer-Tropsch synthesis with supported ruthenium catalysts: (1) CO can react with Ru to form ruthenium carbonyl; (2) CO can react with H_2 to yield hydrocarbons and H_2O;

and (3) CO can react with H_2O to form H_2 and CO_2 [6]. The selectivity for each of these reactions, the olefin-to-paraffin ratio, and the chain growth probability in hydrocarbon synthesis were found to be influenced by the ruthenium metal particle size in the fresh alumina-supported catalysts. This report speculated that these particle size effects may be explained by differences in the ease with which CO can be dissociated over smaller and larger ruthenium particles.

In this new study, the Fischer-Tropsch behavior of two catalysts from the earlier work by Abrevaya et al., a highly dispersed ruthenium catalyst and a catalyst with 3–7 nm ruthenium particles, was correlated with the ability of these catalysts to dissociate the CO molecule.

2. Experimental

CATALYST PREPARATION

The two catalysts were prepared on the same γ-alumina support. Before impregnation with ruthenium-containing solutions, the support was ground to a size range of 60 to 100 mesh.

A highly dispersed ruthenium catalyst was prepared by evaporative impregnation using an aqueous solution of ruthenium nitrosyl chloride (from Alfa Products). The impregnated catalyst was later calcined with air at 300 °C in a fluidized bed. After calcination, the catalyst was cooled in air to 40 °C and then purged with N_2. The catalyst was next heated in H_2 flow to 500 °C and reduced for two more hours in H_2. The reduced catalyst was cooled in H_2 to room temperature and purged with N_2 before unloading in a glove bag. The catalyst was then transferred to a bottle and sealed within the glove bag.

The second ruthenium catalyst was prepared by impregnation with a reverse micelle solution of ruthenium nitrosyl chloride, as described in U.S. Patent 4,714,692 [7]. The finishing procedure for this catalyst was the same as that used for the highly dispersed catalyst except for a 380 °C reduction temperature.

CATALYST TESTING

The catalysts were loaded into a glass-lined, fixed-bed reactor in reduced form under N_2. The temperature was then raised under H_2 flow at 101 kPa to 208 °C at the inlet of the catalyst bed. The reactor was then pressurized with He to 5 MPa for a 1-hour pressure test. Following the pressure test, the pressure was lowered to 3.5 MPa, and the feed was introduced. The feed was a premixed blend of 63.0% H_2, 31.5% CO, and 5.5% Ar.

Similar catalyst-bed temperatures could be obtained at about the same space velocity when less of the more active catalyst and more of the less active catalyst were used. Accordingly, the catalyst volumes were 29 cc for the catalyst with 3–7

nm ruthenium particles and 61 cc for the highly dispersed ruthenium catalyst. For these two catalysts, the gas hourly space velocities were 125 hr^{-1} and 140 hr^{-1}, respectively.

Argon was used as an internal standard for calculating catalytic performance according to the following expressions:

$$CO + H_2 \text{ conversion, } \% = \frac{(CO + H_2/Ar)_{feed} - (CO + H_2/Ar)_{product}}{(CO + H_2/Ar)_{feed}} \times 100$$

$$CO_2 \text{ selectivity, } \% = \frac{(CO_2/Ar)_{product}}{(CO/Ar)_{feed} - (CO/Ar)_{product}} \times 100$$

$$C_1 \text{ selectivity, } \% = \frac{(CH_4/Ar)_{product}}{(CO/Ar)_{feed} - (CO/Ar)_{product}} \times \frac{100}{100 - CO_2 \text{ selectivity}} \times 100$$

$$H_2 : CO \text{ usage ratio} = \frac{H_2 \text{ conversion, } \%}{CO \text{ conversion, } \%} \times H_2 : CO \text{ molar feed ratio.}$$

The calculations of H_2 and CO conversions were similar to the calculation for $CO + H_2$ conversion.

SCANNING TRANSMISSION ELECTRON MICROSCOPY (STEM)

The sample preparations were done under N_2. The catalysts were ground to a fine powder with a mortar and pestle. The powder was deposited on a holey carbon-coated nylon grid which was treated with a drop of isopropanol. The excess powder was removed from the grid by gentle tapping. While under N_2, the specimen was put into the cartridge and placed into the HB-5 STEM. This procedure was accomplished by transfer of the specimen in a N_2-purged glove bag to the sample delivery chamber of the HB-5, which was also purged with N_2. After the transfer was completed, the top of the HB-5 delivery chamber was put in place, the sample evacuated to 10^{-9} Torr, and the catalysts examined.

GAS ADSORPTION

Oxygen chemisorption and H_2 titration of oxygen chemisorbed on ruthenium were used for determining the relative ruthenium metal dispersion for the catalysts. Each catalyst was treated with H_2 at 380 °C for 1 hour, purged with helium for 15 minutes at 380 °C, and cooled to room temperature in helium. Pulses of oxygen were introduced over the catalyst, and the amount of uptake was determined. The catalyst was then heated in helium to 50 °C. Pulses of H_2 were then introduced over the catalyst. Chemisorbed oxygen was typically unreactive at 50 °C, and accordingly, the amount of H_2 uptake was low. The catalyst was then heated in helium to 375–380 °C and further pulsed with H_2. Most of the H_2 uptake occurred under these conditions. Additional H_2 uptake at 500 °C was low.

The oxygen uptake or the total hydrogen uptake was then taken to be proportional to the ruthenium surface area.

For CO disproportionation measurements, each reduced ruthenium catalyst was loaded to the sample cell under N_2. Before the measurements were made, the catalyst sample was heated in H_2 at 380 °C for 1 hour. The catalyst was then purged with He and cooled under He to 208 °C, which is the temperature at which Fischer-Tropsch synthesis was conducted. The CO was then pulsed over the catalyst under 40 cc/min He flow, and the disappearance of CO and the appearance of CO_2 were monitored by a quadrupole mass spectrometer (QMS) and a thermal conductivity detector. Several CO pulses were introduced about every 10 minutes until no further CO uptake occurred. After the CO pulses, a H_2 pulse was introduced, and the amount of CH_4 was determined by QMS.

The percent of CO dissociation efficiency was determined by dividing the amount of CO_2 desorbed by half of the total CO adsorbed. This calculation is based on the stoichiometry of the CO disproportionation reaction:

$$2CO \rightarrow C + CO_2.$$

EXAFS

The EXAFS measurement was done with the highly dispersed ruthenium catalyst at Brookhaven National Laboratory in the fluorescence mode. The reduced catalyst was heated with H_2 at 380 °C and transferred to a sealed copper cell under H_2 just prior to EXAFS measurements.

3. Results

RUTHENIUM METAL DISPERSION

The results for oxygen chemisorption and for titration of chemisorbed oxygen with hydrogen for the two catalysts are shown in table 1. The reproducibility of these measurements is ±8%. The same table also shows the catalyst compositions.

Table 1
Catalyst properties

% Ru (by wt.)	% Cl (by wt.)	O : Ru	H_2 : Ru	Percent of total H_2 uptake		
				50 °C	380 °C	500 °C
1.05	1.0	1.1	1.1	8%	79%	13%
1.12	0.5	0.55	0.50	12%	84%	4%

The chemisorbed oxygen : ruthenium molar ratio was 1.1 with the highly dispersed ruthenium catalyst. The amount of chemisorbed oxygen was two times less over the catalyst with 3–7 nm ruthenium particles. In each case, most of the hydrogen uptake occurred at 380 °C. For both catalysts, the total molar hydrogen uptake was twice as high as than the molar oxygen uptake. These results suggest that the approximate reaction stoichiometry is:

$$Ru + \tfrac{1}{2}O_2 \rightarrow RuO$$

$$RuO + H_2 \rightarrow Ru + H_2O.$$

Following the titration of chemisorbed oxygen, little if any, hydrogen is adsorbed on ruthenium. At 50 °C, hydrogen can not adsorb on ruthenium in significant quantities because of the presence of a large amount of unreactive oxygen. At 380 °C and 500 °C, net hydrogen adsorption on ruthenium may be prohibited because of the high temperature.

RUTHENIUM METAL AGGLOMERATION

The STEM micrograph of the highly dispersed ruthenium catalyst on alumina is shown in fig. 1. The absence of visible ruthenium particles indicates that ruthenium is in the form of aggregates, which are smaller than 2 nm. In fact, according to EXAFS, the ruthenium particle size in this catalyst is about 0.8 nm [6]. Furthermore, the gas adsorption measurements, which show the O : Ru ratio to be 1.1, confirms that the ruthenium particles were small and that probably all of the Ru atoms were exposed.

Fig. 1 also shows the STEM micrograph of the same catalyst after it was subjected to 12 hours of synthesis gas at 208 °C. The catalytic performance during this test is described in the next section. The catalyst was examined by STEM after the test. The results indicate that slightly less than a quarter of the alumina particles still had ruthenium in the highly dispersed form. The rest of the alumina particles contained, in about equal number, particles that were 3–8 nm and particles that were 10–25 nm.

The Fourier transform of EXAFS oscillations of the highly dispersed ruthenium catalyst before and after Fischer-Tropsch synthesis are compared in fig. 2. The peaks at distances larger than 0.2 nm are associated with Ru-Ru nearest neighbor and higher neighbor coordinations. The increase in the amplitude of these peaks after the test indicates that the average coordination number has significantly increased, confirming that ruthenium particles agglomerated to larger sizes. The EXAFS curve-fitting results for Ru nearest neighbors are summarized in table 2.

During Fischer-Tropsch synthesis tests with highly dispersed ruthenium catalysts, ruthenium carbonyl in the form of $Ru_3(CO)_{12}$ was always detected in the cold product receivers at the outlet of the reactor. Analyses of ruthenium on the catalysts before and after the tests indicated overall ruthenium loss from catalysts. For example, in this test, the ruthenium level in the catalyst decreased from

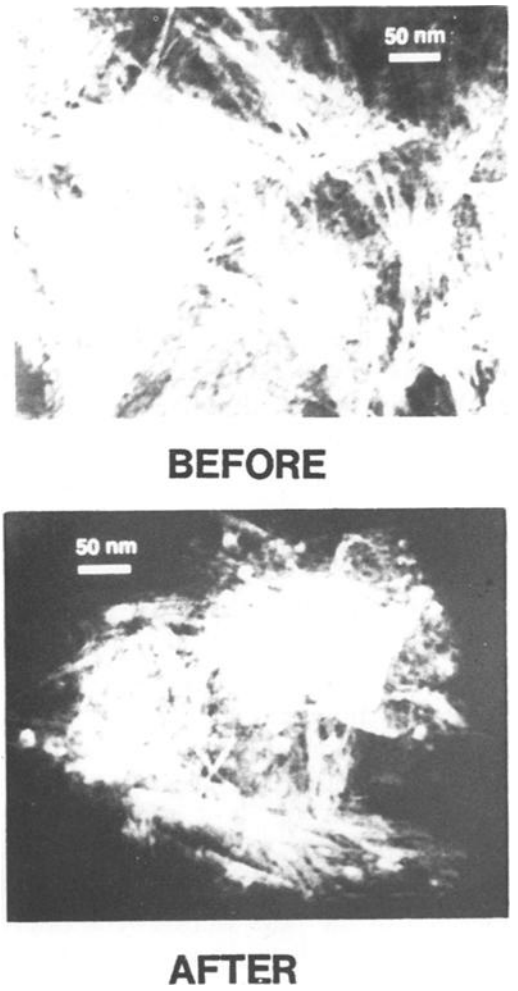

Fig. 1. STEM micrographs of highly dispersed ruthenium catalysts on alumina before and after Fischer-Tropsch synthesis.

1.05% to 0.80% in a matter of 12 hours. These results indicate that highly dispersed ruthenium was not stable on alumina during Fischer-Tropsch synthesis. Highly dispersed ruthenium migrated on the catalyst surface via the formation of a volatile ruthenium carbonyl species and formed larger ruthenium particles. The formation of the volatile carbonyl species also caused overall ruthenium loss from the catalyst.

The STEM micrograph of the reverse micelle-derived fresh catalyst is shown in fig. 3. About 85% of the ruthenium particles in this catalyst were 3–7 nm; the rest were 7–10 nm. As opposed to highly dispersed ruthenium, agglomeration was mild, with 3–7 nm ruthenium during Fischer-Tropsch synthesis. The particle size

Table 2
EXAFS-curve fitting results

	Bond length (nm)	Disorder parameter ($\times 10^{-3}$)	Coordination number
Before Fischer-Tropsch	0.261	2.08	3.4
After Fischer-Tropsch	0.265	1.17	13.6

range was mostly 4–7 nm at the end of the test. With other catalysts having 4–6 nm ruthenium particles, agglomeration was not observed. These results indicate that 4 nm was the threshold size for maintaining the ruthenium particle size during Fischer-Tropsch synthesis.

The catalyst with 4–6 nm ruthenium particles did not form ruthenium carboxyl during Fischer-Tropsch synthesis. This result was confirmed by chemical analysis of the used catalyst. The analysis indicated no overall ruthenium loss from the catalyst.

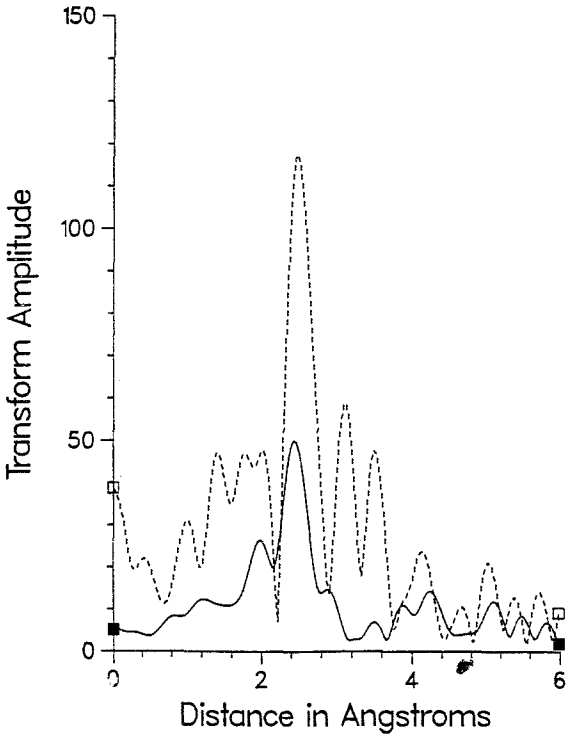

Fig. 2. Ru-Ru phase and amplitude corrected Fourier transforms of the highly dispersed ruthenium on alumina catalyst before (■) and after (□) Fischer-Tropsch synthesis.

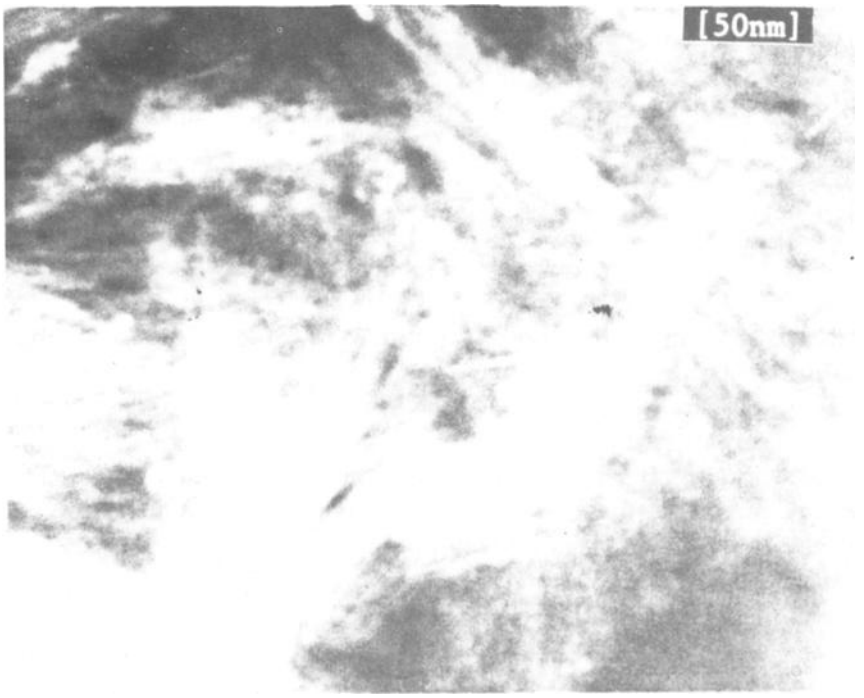

Fig. 3. STEM micrograph of the catalyst with 3–7 nm ruthenium particles.

CATALYTIC ACTIVITY AND SELECTIVITY

The catalyst with the larger ruthenium particles was tested at 63 hr^{-1} space velocity during the first 25 hours on-stream. For comparison to the highly dispersed ruthenium catalyst, the space velocity was then increased to 125 hr^{-1} for the catalyst with 3–7 nm ruthenium and maintained at this rate for 10 hours. The catalytic behavior of this catalyst was then compared in fig. 4 to the highly dispersed catalyst that was tested at 140 hr^{-1}.

The $CO + H_2$ conversion, which is indicative of the hydrocarbon synthesis activity, increased from 8 to 11% during the test with the highly dispersed ruthenium catalyst. The $CO + H_2$ conversion ranged between 16 and 18% with the catalyst having 3–7 nm ruthenium particles. The lower activity over the highly dispersed ruthenium catalyst prior to significant ruthenium agglomeration indicates that the ruthenium catalyst has a lower turnover number for hydrocarbon synthesis relative to 3–7 nm ruthenium particles. Ruthenium agglomeration during the test with the highly dispersed catalyst is expected to cause both an increase in the turnover number as well as a decrease in the number of exposed Ru atoms. The slight increase in the activity of the highly dispersed catalyst with time on-stream suggests that the first effect may have overridden the second effect, resulting in increased overall activity.

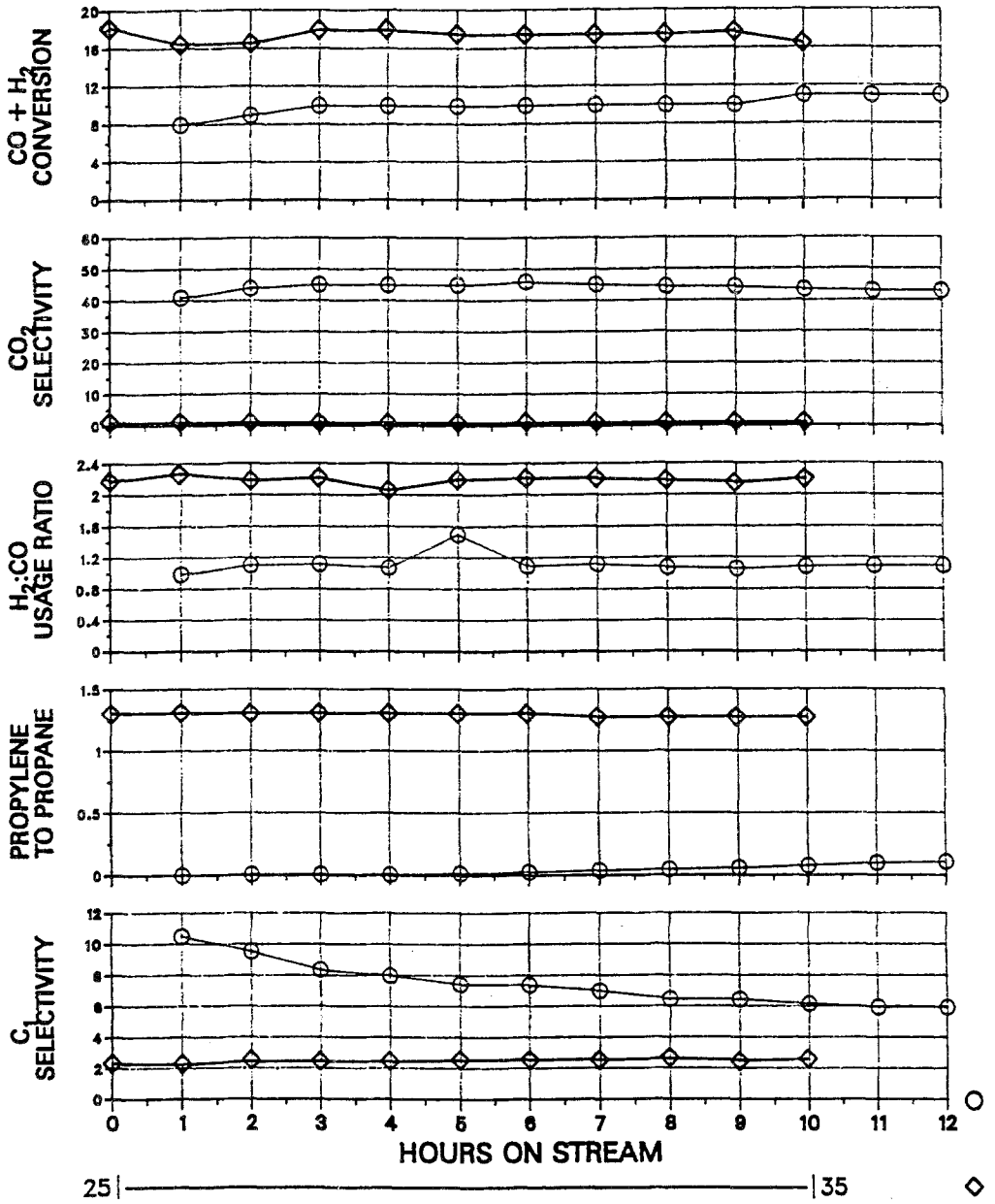

Fig. 4. Activity and selectivity differences in Fischer-Tropsch synthesis between highly dispersed ruthenium catalyst (○) and the catalyst with 3–7 nm ruthenium particles (◇).

Highly dispersed ruthenium showed 40–45% selectivity to CO_2. The ratio of H_2 and CO consumption was 1.1. The CO_2 selectivity was less than 2% with the catalyst having 3–7 nm ruthenium particles and, therefore, slightly more than two moles of H_2 were consumed for every mole of CO. The persistent nature of high

CO_2 selectivity with the highly dispersed ruthenium catalyst despite ruthenium metal agglomeration suggests that the presence of a small remaining amount of highly dispersed ruthenium is sufficient to cause the CO_2 production.

The propylene to propane ratio was < 0.1 for the highly dispersed ruthenium catalyst. The catalyst with 3–7 nm ruthenium particles showed a higher propylene to propane ratio of about 1.3. The significance of these results is discussed in the last section.

The hydrocarbon selectivity to methane decreased from about 10 to 6% during the test with the highly dispersed ruthenium catalyst. The result indicates an increase in the selectivity to higher hydrocarbons and an increase in the chain-growth probability accompanying ruthenium agglomeration. As expected, the 2.5% selectivity to methane was much lower with 3–7 nm ruthenium particles.

CO DISPROPORTIONATION

Two measurements were performed with the highly dispersed catalyst. For the first measurement a total of 18 CO pulses were introduced over the catalyst. The amount of CO in each of the first 15 pulses was equal to 0.05 cc. The 16th, 17th and 18th pulses were larger: 0.25 cc. The second measurement with the highly dispersed ruthenium catalyst was identical to the first one except only 16 pulses were used. All 12 CO pulses over the catalyst with 3–7 nm ruthenium were 0.05 cc.

Over the highly dispersed ruthenium catalyst, the first five CO pulses were totally consumed with no CO_2 detection. The CO_2 was detected after the fifth pulse. Over the catalyst with 3–7 nm ruthenium particles, the first three CO pulses were totally consumed, resulting in a small amount of CO_2 desorption. Larger amounts of CO_2 were observed with increased number of pulses. With both catalysts, no measurable time delay occurred between the detection of unadsorbed CO and desorbed CO_2, which indicates that the CO disproportionation reaction was rapid.

The cumulative amounts of CO adsorbed, CO_2 desorbed, CO dissociation efficiencies, and the amounts of CH_4 desorbed for the two catalysts are shown in table 3.

Table 3
Cumulative CO disproportionation results

	μ Mol Ru / g cat	μ Mol CO / g cat.	CO : Ru	μ Mol CO_2 / g cat.	CO dissociation efficiency	μ mol CH_4 / g cat.
Highly dispersed Ru	104	90	0.87	0.61	1.3%	85–88 (208° C)
		88	0.85	0.61	1.4%	0.55 (25° C)
3–7 nm Ru	111	57	0.51	1.98	6.9%	53–55 (208° C)

The overall CO dissociation efficiency was 1.3–1.4% for the highly dispersed catalyst and 6.9% for the catalyst with 3–7 nm particles. These overall CO dissociation efficiencies are three to four times lower than the efficiencies obtained with each of these catalysts at high coverage before saturation of the surface with CO. The cumulative amount of CO uptake per mole of ruthenium was 0.86 ± 0.01 over the highly dispersed ruthenium catalyst and 0.51 over the catalyst with 3–7 nm ruthenium particles.

With both catalysts, the amounts of methane detected at 208°C after the H_2 pulses (0.25 cc each) following CO disproportionation measurements, were 92–97% of the total amount of carbon on the catalyst surface. These results indicate that, at 208°C, H_2 reacted with most of the adsorbed CO to make CH_4. Because carbon deposited during CO disproportionation was much less than the amount of CO adsorbed, no determination of whether surface carbon reacted with H_2 could be made. To titrate the amount of surface carbon deposited during the second CO disproportionation measurements with the highly dispersed ruthenium catalyst, the temperature was lowered to 25°C under He flow, and H_2 was pulsed. At 25°C, adsorbed CO is not expected to react with H_2. In this experiment, the amount of CH_4 corresponded to 90% of the carbon deposited, as calculated, from the amount of CO_2 desorbed during CO disproportionation. These results indicate that carbon resulting from CO disproportionation is more reactive toward H_2 than undissociated CO. Therefore, the catalyst with higher CO dissociation efficiency is expected to be more active during Fischer-Tropsch synthesis.

4. Discussion

Rabo et al. previously reported CO pulsing experiments with supported Ru, Co, Ni, and Pd catalysts to determine whether CO adsorption is dissociative over these metals [8]. They found that on all metals studied, except for Pd, CO adsorption was dissociative at 300–400°C. Similar experiments were conducted in this work to compare CO dissociation efficiencies with a highly dispersed ruthenium on alumina and an alumina-supported catalyst with mostly 3–7 nm ruthenium particles at 208°C, which is the temperature at which these catalysts were tested for Fischer-Tropsch synthesis.

Differences in the catalytic behavior of highly dispersed and 3–7 nm ruthenium on alumina support during Fischer-Tropsch synthesis can be attributed to differences in the effectiveness of these catalysts to dissociate the CO molecule. In this study, CO dissociation efficiency was found to be much higher over 3–7 nm ruthenium particles than over highly dispersed ruthenium on alumina. The CO dissociation requires a large ensemble of metal atoms [9] and, therefore the probability of finding an ensemble of available metal atoms is less with smaller particles. Because carbon resulting from CO dissociation is more reactive toward

H_2 than undissociated CO, the lower turnover number observed for smaller particles can be attributed to the lower CO dissociation efficiency. Furthermore, low CO dissociation efficiency implies that the relative abundance of CH_2 surface species responsible for chain growth will be low relative to surface hydrogen, which is responsible for chain termination. This implication would make the chain growth probability lower with the highly dispersed ruthenium catalyst, which is also what is observed in this study.

The relative ineffectiveness of the highly dispersed ruthenium in dissociating the CO molecule opens the possibility that reactions that do not require CO dissociation may be enhanced. One such example is the tendency toward enhanced ruthenium carbonyl formation observed with the highly dispersed ruthenium. This ruthenium carbonyl formation led to ruthenium agglomeration during Fischer-Tropsch synthesis.

While CO disproportionation reaction occurs over 3–7 nm ruthenium particles in the absence of H_2, CO_2 is not formed in any significant amount during Fischer-Tropsch synthesis. Over 3–7 nm ruthenium particles, the approximate reaction stoichiometry is in fact:

$$n\mathrm{CO} + 2n\mathrm{H_2} \rightarrow (\mathrm{CH_2})_n + n\mathrm{H_2O}.$$

The absence of CO_2 formation over 3–7 nm ruthenium particles during Fischer-Tropsch synthesis indicates the removal of CO dissociation product surface oxygen, O_s (where s designates surface), with surface hydrogen, H_s, is kinetically more favored than the removal of O_s with CO_s.

However, CO_2 can also form by the water-gas shift reaction between Fischer-Tropsch product water and carbon monoxide. According to bond-order conservation calculations at zero coverage by Shustorovich, the reaction between adsorbed CO and surface hydroxyl to give CO_2 and surface hydrogen has low activation energy [10].

$$\mathrm{CO_s} + (\mathrm{OH})_s \rightarrow (\mathrm{CO_2})_s + \mathrm{H_s} \quad E_a = 4 \text{ kcal/mole}.$$

The fact that this easy reaction does not occur significantly over 3–7 nm ruthenium particles can be explained by the absence of surface hydroxyls. If the removal of surface oxygen by hydrogen occurs in one elementary step without the intermediate formation of surface hydroxyls, then water dissociation becomes the only source of hydroxyls. The nonoccurrence of water dissociation over 3–7 nm ruthenium particles may then explain the virtual absence CO_2 in the products.

Over highly dispersed Ru, CO_2 is formed in significant quantities. The CO_2 can form either directly during Fischer-Tropsch synthesis when surface oxygen is removed by carbon monoxide rather than by hydrogen, according to the approximate reaction stoichiometry:

$$2n\mathrm{CO} + n\mathrm{H_2} \rightarrow (\mathrm{CH_2})_n + n\mathrm{CO_2}.$$

The CO_2 can also form by the water-gas shift reaction, following the Fischer-Tropsch reaction favoring H_2O:

$$n\mathrm{CO} + 2n\mathrm{H_2} \rightarrow (\mathrm{CH_2})_n + n\mathrm{H_2O}$$
$$n\mathrm{CO} + n\mathrm{H_2O} \rightarrow n\mathrm{CO_2} + n\mathrm{H_2}$$
$$2n\mathrm{CO} + n\mathrm{H_2} \rightarrow (\mathrm{CH_2})_n + n\mathrm{CO_2}$$

Distinguishing between these two mechanisms is not always possible. However, examination of product selectivities with highly dispersed ruthenium catalysts at different space velocities show that CO_2 selectivity increases with an increase in the conversion level, which strongly suggests that CO_2 is not a primary but a secondary reaction product originating from the water-gas shift reaction. The same conclusion was also reached by Anderson in the case of iron Fischer-Tropsch catalysts [11]. The results then, suggest that highly dispersed ruthenium has sites that are effective in H_2O dissociation.

Because the water-gas shift reaction is the most likely source of CO_2 over highly dispersed ruthenium catalyst, the low olefinicity of hydrocarbons observed with the highly dispersed ruthenium catalyst can be attributed to the in situ generation of H_2, which would result in a high H_2 virtual pressure. The in situ generation of H_2 also partly explains the lower chain growth probability observed with highly dispersed ruthenium catalyst. However, as discussed previously, intrinsic particle size effects also seem to influence chain growth probability [6].

Acknowledgment

The authors would like to thank the U.S. Department of Energy for providing the funds for doing this work and Dr. E. Shustorovich for his helpful discussions.

References

[1] M. Boudart and M.A. McDonald, J. Phys. Chem. 88 (1984) 2185.
[2] C.S. Kellner and A.T. Bell, J. Catal. 75 (1982) 251.
[3] T. Fukushima, K. Fujimoto and H. Tominaga, Appl. Catal. 14 (1985) 95.
[4] D.L. King, J. Catal. 51 (1987) 386.
[5] T. Okuhara, T. Kimura, K. Kobayashi, M. Mishono and Y. Yoneda, Bull. Chem. Soc. Jpn. 57 (1984) 938.
[6] H. Abrevaya, W.M. Targos, H.J. Robota and M.J. Cohn, 10th N. American Meeting of the Catalysis Society, San Diego, CA., ed. J.W. Ward, Catalysis (1987) 97.
[7] H. Abrevaya and W.M. Targos, UOP, U.S. Patent 4,714,692.
[8] J.A. Rabo, A.P. Risch and M.L. Poutsma, J. Catal. 53 (1978) 295.
[9] V. Ponec and W.A. Van Barneveld, Ind. Eng. Chem. Prod. Res. Dev. 18 (1979) 268.
[10] E. Shustorovich, private communication, to appear in Advances in Catalysis 37 (1990) 99.
[11] R.B. Anderson, *The Fischer-Tropsch Synthesis* (Academic Press, New York, 1983).